

Hybrid One-Dimensional Nanostructures: One-Pot Preparation of Nanoparticle Chains via Directed Self-Assembly of in Situ Synthesized Discrete Au Nanoparticles

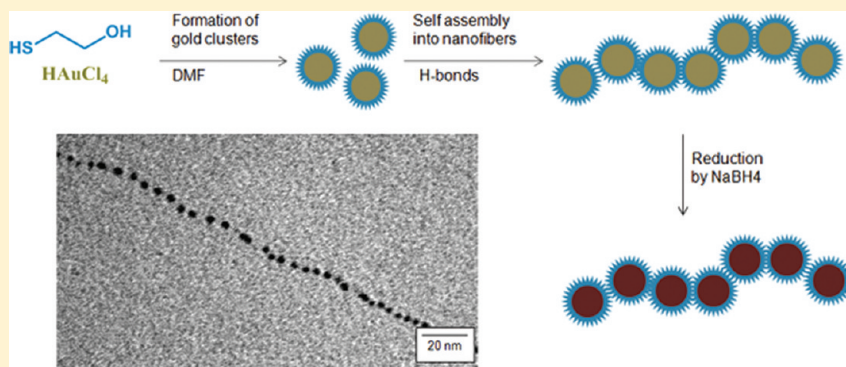
Marie V. Walter,[†] Nicolas Cheval,[‡] Olimpia Liszka,[‡] Michael Malkoch,^{*,†} and Amir Fahmi^{*,‡,§}

[†]School of Chemical Science and Engineering, Department of Fibre and Polymer Technology, KTH Royal Institute of Technology, SE-100, 44 Stockholm, Sweden

[‡]Division of Mechanical, Materials and Manufacturing Engineering, University of Nottingham, NG7 2RD, United Kingdom

[§]Faculty of Technology and Bionics, Rhein-Waal University of Applied Sciences, Nollenburgerweg 115, D-46446 Emmerich, Germany

Supporting Information



ABSTRACT: The fabrication of well-defined one-dimensional (1D) arrays is becoming a challenge for the development of the next generation of advanced nanodevices. Herein, a simple concept is proposed for the in situ synthesis and self-assembly of gold nanoparticles (AuNPs) into 1D arrays via a one-step process. The results demonstrated the formation of nanoparticle chains (NPC) with high aspect ratio based on discrete Au nanoparticles stabilized by short thiol ligands. A model was proposed to explain the self-assembly based on the investigation of several parameters such as pH, solvent, temperature, and nature of the ligand on the 1D assembly formation. Hydrogen bonding was identified as a key factor to direct the self-assembly of the hybrid organic–inorganic nanomaterials into the well-defined 1D nanostructures. This simple and cost-effective concept could potentially be extended to the fabrication of a variety of hybrid 1D nanostructures possessing unique physical properties leading to a wide range of applications including catalysis, bionanotechnology, nanoelectronics, and photonics.

INTRODUCTION

Self-assembly is a widely used technique in the field of nanotechnology to access ordered macroscopic 1D, 2D, or 3D structures from simple building blocks such as nanorods and/or nanoparticles (NP).^{1–4} Recently, the attention paid to one-dimensional (1D) nanomaterials has been increasing significantly because of the need to fabricate alternative functional 1D nanostructures for applications in the fields of nanoelectronics and nanobiotechnology.^{5–8} The appeal of 1D nanostructures derives from their intrinsic properties: these are the smallest structures capable of efficiently transporting electrical carriers and can therefore be used both as wiring or device elements in the design of the new generation of miniaturized devices. From the family of 1D nanostructures, organic,^{9–11} organometallic,^{12,13} and organic–inorganic hybrid structures¹⁴ are particularly attractive because of their chemically tunable properties and facilities for solution processing.

Electrospinning is a versatile technique for the production of 1D arrays. This technique permits the fabrication of fibers from natural or synthetic polymer fibers as well as from ceramics and metals down to a few nanometers in diameter. These nanofibers can be loaded with various agents such as chromophores, and nanoparticles offering the advantages of bringing new functionalities to the organic matrix.¹⁵ The structural properties of the nanofibers, such as shape and diameter, depend on a variety of chemical parameters including molecular weight, solubility, glass transition temperature (T_g) of the polymer, and concentration, viscosity or surface tension of the polymer solution, as well as processing parameters such as feed rate of the solution or geometry of the electrodes.

Received: January 4, 2012

Revised: March 11, 2012

Published: March 20, 2012



Fabrication of nanofibers requires therefore the optimization of these parameters, often leading to a narrow operating window. Consequently, the concept is complex to implement and the diameters of the obtained nanofibers are seldom uniform.¹⁶

Another approach to obtain 1D arrays is via the self-assembly of anisotropic particles. In the case of spherical nanoparticles, controlling the surface chemistry of the fabricated nanoparticles allows the creation of an anisotropic ligand organization. This facilitates the orientation of specific interactions in one direction, which helps directing the self-assembly into 1D arrays. This concept was successfully exploited by Stellaci and co-workers¹⁷ who introduced anisotropic properties on ligand stabilized AuNPs. The ligands situated at the poles of a particle are less stabilized by intermolecular interactions than their neighbors and are therefore the first to be replaced during ligand-exchange reactions. These pole-modified NPs were then employed as building blocks to generate nanoparticle chains (NPC). The self-assembly of the NPs into a well-defined 1D array is also influenced by interparticle chemical bonding, hydrogen bonding, van der Waals interactions, electrostatic forces, or any combination of these forces. For instance, Wang and co-workers demonstrated that in the case of negatively charged thioglycolic acid capped nanoparticles, the electrostatic repulsion experienced by a particle attaching to the end of a particle chain is weaker than for a side of chain attachment.^{18,19} However, the self-assembly process is limited by the stability of the nanoparticles in solution since particles at the nanoscale level have a high tendency to undergo self-aggregation. Therefore, the self-assembly of uncharged nanoparticles with size below 5 nm in solution is difficult to achieve.^{20,21}

Gold nanoparticles (AuNPs) have been intensively investigated over the past few years with respect to their synthesis and self-assembly.^{22–27} The specific properties of AuNPs make them of utmost interest for applications in electronics, optics, catalysis, or medicine.^{28–32} AuNPs can be synthesized through various methodologies, the most common one being the citrate reduction of HAuCl₄ in water, introduced by Turkevich et al. in 1951.³³ The use of citrate permits a controlled ligand exchange of the ions adsorbed on the surface. Another interesting route is the Brust–Schiffrin method, using thiol ligands that strongly bind to gold to stabilize the particles.³⁴ The obtained particles can in this case be isolated and redissolved in organic solvents, enabling further functionalization through conventional organic chemistry. Moreover, the particle size and polydispersity can easily be controlled by varying the thiol to gold ratio or the reduction conditions.^{28,35} It has already been reported that citrate decorated gold-nanoparticles could assemble into nanofibers after partial ligand exchange of the adsorbed citrate ions by mercaptoethanol (MEA) or thioglycolic acid.^{18,36} This spontaneous assembly is attributed to the electric dipole formed by the anisotropic organization of the ligands on the surface of the NP.³⁷ However, to our knowledge, self-assembly of in situ synthesized nanoparticles in nonaqueous medium employing a one-pot methodology and using only commercially available compounds has not yet been reported.

Herein, we investigate several commercially available thiol building blocks to direct the assembly of in situ synthesized gold NPs into 1D nanoparticles chains (NPC) via a cost-effective one step self-assembly process. Moreover, the effect of critical parameters such as molar ratio, pH, temperature, and solvent on the NPC formation is examined. The NPC systems were characterized by means of atomic force microscopy (AFM), transmission electron microscopy (TEM), high

resolution TEM, and attenuated total reflection Fourier transformed Infrared spectrometry (ATR-FTIR).

EXPERIMENTAL SECTION

Materials. Dimethylformamide (DMF) and dimethyl sulfoxide (DMSO) were purchased from Fisher Scientific. Cysteamine (>98%) was purchased from Fluka. Hydrogen tetrachloroaurate (HAuCl₄) (99.9%), 2-mercaptopropanoic acid (MPA) (>99%), and 11-mercaptopropionic acid (MU) (99%) were purchased from Sigma-Aldrich. 2,2-Bis(hydroxymethyl)-2-mercaptopropanoate (BMP) was purchased from Polymer Factory Sweden AB.

Instrumentation. TEM measurements were performed using a TECNAI Biotwin (FEI Ltd.) at 100 keV to determine the size and size distribution of particles. The instrument was operated at low beam intensities to prevent electron damage of the polymer samples. Hybrid materials solutions were deposited on carbon-coated copper grids (400 meshes, AGAR Scientific). Atomic force microscopy (AFM) (Digital Instruments Dimension 3100 Nanoscope) with Si cantilevers (Nanoworld Point Probe Cantilevers, $f = 315$ kHz, $k = 40$ N/m) was used to investigate the film morphology of the samples. The measurements were performed in tapping mode to minimize any damage to the sample surface. UV-vis spectra were recorded using a Varian Cary 50 photospectrometer (Varian Inc.) with the monochromator slit width of 5 mm. Spin-coating was performed on a DELTA 10 TT spincoater (SÜSS Microtec lithography GmbH) at 2500 rpm for 10 s, depositing one drop of solution on the substrate (0.5 × 1 cm). Plasma etching was performed in a Plasma system femto (Diener electronic) under oxygen atmosphere for 20 min. An attenuated total reflection fourier transform infrared instrument from Bruker (model Tensor 27) was used at ambient temperature in the spectral range from 4000 to 550 cm⁻¹.

Cleaning of the Silicon Substrates. The silicon wafers were first cleaned with acetone and water. Thereafter, a second cleaning was performed with a piranha solution. The wafers were immersed in a H₂SO₄/H₂O₂ (4:1) solution at 70 °C for 15 min, rinsed with water, and immersed again in a H₂O₂/NH₃/H₂O (1:1:1) solution at 60 °C for 15 min. The surfaces were finally rinsed with water and dried under nitrogen flow. Warning: Piranha solution reacts strongly with organic compounds and should be handled with extreme care.

Preparation of Gold Nanoparticles. A solution of thiol ligands was prepared at 1 mg/mL in DMF. Hydrogen tetrachloroaurate (0.2 equiv to thiol ligand) was added to the solution and stirred overnight. The gold precursor was then reduced to form gold nanoparticles using sodium borohydride (10 equiv to HAuCl₄, in water), resulting in a color change of the solution from slightly yellow to dark red.

RESULTS AND DISCUSSION

The formation of nanofibers via the self-assembly of AuNPs is usually performed in two steps: synthesis of AuNPs followed by ligand exchange to induce the self-assembly. In this section, a novel concept is proposed to synthesize and in situ self-assemble AuNPs into well-defined 1D nanostructures via a one-pot chemical process.

The method relies on the synthesis of AuNPs in a one-phase system in the presence of thiols. In this study, the potential of several commercial thiols to direct the in situ assembly of AuNPs into nanofibers is investigated. The thiol monomers were chosen to evaluate the influence of several parameters on the formation of fibers such as the nature of the functional groups, the length of the alkyl backbones, and the introduction of branching. The investigation was based on linear hydroxyl terminated thiols, 2-mercaptopropanoic acid (MEA) and 11-mercaptopropionic acid (MU), as well as a dihydroxyl terminated thiol, 2,2-bis(hydroxymethyl)-2-mercaptopropanoate (BMP). The presence of the hydroxyl group was expected to favor the self-assembly via the formation of hydrogen bonds. MU was

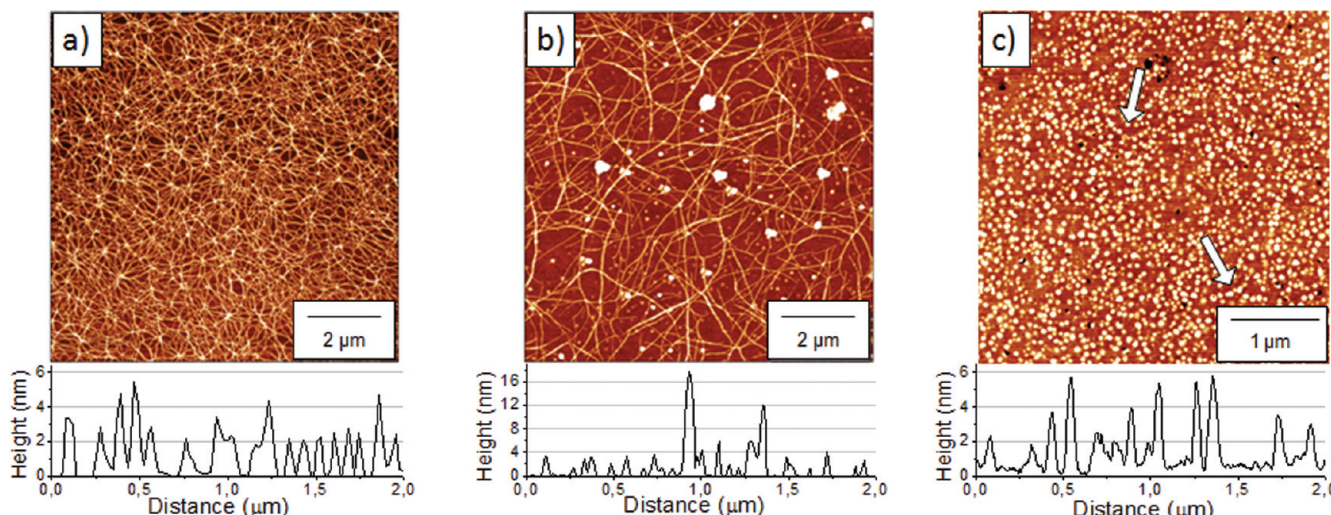


Figure 1. (a) AFM height image and surface profile of MEA/HAuCl₄ (molar ratio of 5 to 1). (b) AFM height image and surface profile of MEA/HAuCl₄ (molar ratio of 5 to 1) after reduction by NaBH₄. (c) AFM height image and surface profile of MEA/HAuCl₄ (molar ratio of 5 to 1) after oxygen plasma etching.

selected for its longer carbon chain which allows crystallization of the ligands. BMP was chosen to enhance the presence of OH groups. Moreover, an amine and a carboxylic acid functional thiol, cysteamine and 3-mercaptopropionic acid (MPA), respectively, were used to extend the study since both groups can potentially be charged and/or participate in the formation of hydrogen bonds. From the obtained results, a mechanism explaining the formation of NPCs is proposed and confirmed by the evaluation of important parameters such as molar ratio of thiol to gold precursor, solvent, temperature, and pH.

Spontaneous Linear Self-Assembly of in Situ Synthesized Gold Nanoparticles. AuNPs were prepared from hydrogen tetaurochlorate (HAuCl₄) precursor in a one-phase system using DMF as solvent. The polar DMF was chosen because of its ability to efficiently solubilize both the gold precursor and the ligands. Initially, the thiol ligand was dissolved in DMF followed by the addition of HAuCl₄ gold precursor in a molar ratio of 5 mol of thiols for 1 mol of gold precursor. The inorganic precursor dissociates in solution, resulting in [AuCl₄]⁻ complexes that thereafter react with the thiol molecules. The formation of gold nanoparticles is obtained through the addition of a reducing agent (NaBH₄ dissolved in water) to reduce Au³⁺ to Au⁰. Interestingly, when using 2-mercaptoethanol (MEA) as a ligand, 1D nanostructures with high aspect ratio were observed on the solid Si/SiO_x substrate before (Figure 1a) and after (Figure 1b) the reduction of AuNPs. AFM evaluation revealed the formation of 1D nanoarrays in the presence of Au-precursor and MEA, having a diameter of \approx 70 nm with a height of 2–4 nm. However, after reduction of the gold precursor by NaBH₄ in solution, large aggregates were generated. These aggregates probably result from the folding of the 1D arrays from a linear to a globular shape because of disruption of specific interactions between the gold particles and the surrounding solvent. The solution after reduction of the gold precursor was analyzed by UV-vis spectroscopy and showed a maximum absorption at 525 nm, confirming the presence of large gold particles. This value can be attributed to the aggregates, since it has been reported that no plasmon band is observed for AuNPs with core diameter smaller than 2 nm.²⁸

To determine whether the 1D nanostructures resulted from the self-assembly of AuNPs, a substrate coated with the fabricated nanostructures was treated by oxygen plasma etching for 20 min. This treatment permits a selective etching of the organic thiol ligand and reduction of the gold precursor, leaving only the metallic AuNPs on the solid substrate. The AFM height image of the sample after plasma-etching reveals the alignment of particles within the 1D arrays (Figure 1c, white arrows), thus supporting the self-assembly theory of AuNPs into NPCs.

The size and size distribution of the particles were determined by transmission electron microscopy (TEM) measurements on a MEA/HAuCl₄ solution deposited on a copper grid. The emission of electrons during the TEM measurement permits the reduction of the gold precursor. The nanoparticles are observed as dark spots because of their higher density as compared to the organic ligand. The TEM micrographs show the formation of long NPCs with little branching, consisting of monodispersed particles (Figure 2a). The nanoparticles are well-defined with an average diameter of 1.5 nm (Figure 2b). High resolution TEM measurements were conducted to assess the crystalline structure of the particles, as presented in Figure 2c. The characteristic fringes observed via HTREM confirm the monocrystallinity of the particles reduced by the TEM electron beam. The interparticle distance was estimated to 2–4 nm in the linear fibers. However, after reduction of the gold precursor by NaBH₄ in solution, the NPCs tended to aggregate and form large particles, as observed in Figure 2d. The results from the TEM analyses are in agreement with the AFM measurements.

In order to better understand the nature of the interactions involved in the NPCs formation, attenuated total reflection Fourier-transform IR spectroscopy analyses were conducted on pure MEA and a MEA/HAuCl₄ system, before reduction of the gold precursor (see the Supporting Information). The disappearance of the signal at 2554.3 cm⁻¹, corresponding to the vibration of the thiol, after addition of gold precursor confirms the formation of an Au–S bond in the system. Moreover, the appearance of a new signal at 3648 cm⁻¹ and the shift observed for the OH vibration frequency reveal the presence of hydrogen bonds in the fibers.^{38,39}

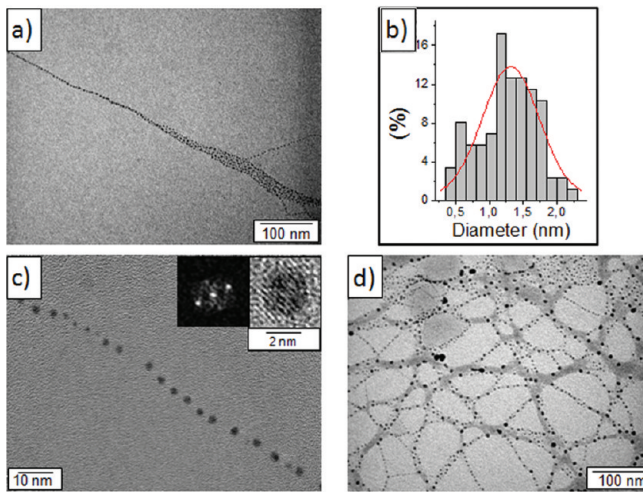


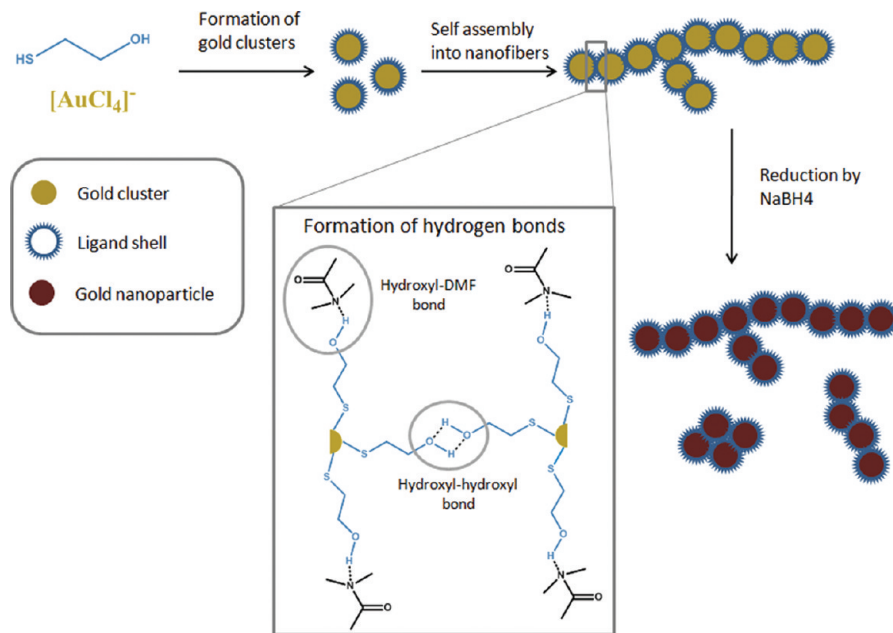
Figure 2. (a) TEM micrograph of gold nanoparticles obtained from MEA/HAuCl₄ (molar ratio of 5 to 1). (b) Size distribution of the gold nanoparticles, obtained from TEM from a solution of MEA/HAuCl₄ (molar ratio of 5 to 1). (c) High resolution TEM micrograph of gold nanoparticles obtained from MEA/HAuCl₄ (molar ratio of 5 to 1). The inserts show the crystalline structure. (d) TEM micrograph of gold nanoparticles obtained from MEA/HAuCl₄ (molar ratio of 5 to 1) after reduction by NaBH₄.

The results obtained suggest that the self-assembly of the nanoparticles into 1D nanoarrays is due to the formation of hydrogen bonds between MEA molecules on one side and between MEA and DMF molecules on the other side. A model is presented in Scheme 1 to explain the formation of nanofibers in solution. It is well reported that S-H groups interact with gold precursor in solution. Upon addition of MEA, gold complexes aggregate to form a gold cluster composed of a gold core surrounded by a thiol ligand shell. At this stage, the gold is still in its oxidized form. Upon addition of a 5 times excess of thiol to the gold precursor, the surface of the gold cluster is saturated by ligands. The clusters can therefore self-assemble

via the formation of hydrogen bonds between the hydroxyl groups of the MEA monomers. The cluster assembly is directed into 1D arrays due to the competitive formation of hydrogen bonds between the hydroxyl group of the MEA and the nitrogen atom of the DMF molecules. Therefore, controlling these two types of interactions is crucial for the formation of 1D nanoarrays. TEM observation and plasma etching of the NPCs reveal the nature of the fibers: the discrete gold nanoparticles self-assemble into a 1D array with a constant interparticle distance. Some irregularities in the spacing are observed when a disulfide bond is formed by oxidation of the MEA, resulting in intercalation between the particles. In DMF, some of the free MEA molecules are oxidized to dihydroxyethyl-disulfide, as confirmed by the appearance of a band at 577 cm⁻¹ in the FTIR spectra (see the Supporting Information). This disulfide forms hydrogen bonds with the hydroxyl groups of two MEA-capped AuNPs and increases the spacing between the Au nanoparticles. Branching occurs when one AuNP participates in more than two interparticle interactions. When the gold is reduced in solution by NaBH₄, some of the fibers fold to form aggregates. The introduction of water into the system disrupts the formation of specific hydrogen bonds between the capped AuNPs. Changing the complementary functional group or the structure of the thiol ligand disrupts the formation of fibers, which indicates the narrow window of potential ligands able to direct the self-assembly of the AuNPs into NPCs. Because of the formation of aggregates after addition of NaBH₄, all the following studies were performed on the ligand/precursor solution in DMF, before reduction of the gold precursor with NaBH₄.

When using the other ligands (MPA, MU, BMP, and cysteamine), no NPCs were formed in solution (see the Supporting Information). The results presented above suggest that the self-assembly of the nanoparticles into 1D nanoarrays is due to the formation of hydrogen bonds between MEA molecules on one side and between MEA and DMF molecules on the other side. In the case of MPA, the carboxylic acid is more susceptible to form hydrogen bonds with the DMF, and

Scheme 1. Proposed Model for the Linear Alignment of Gold Nanoparticles in DMF



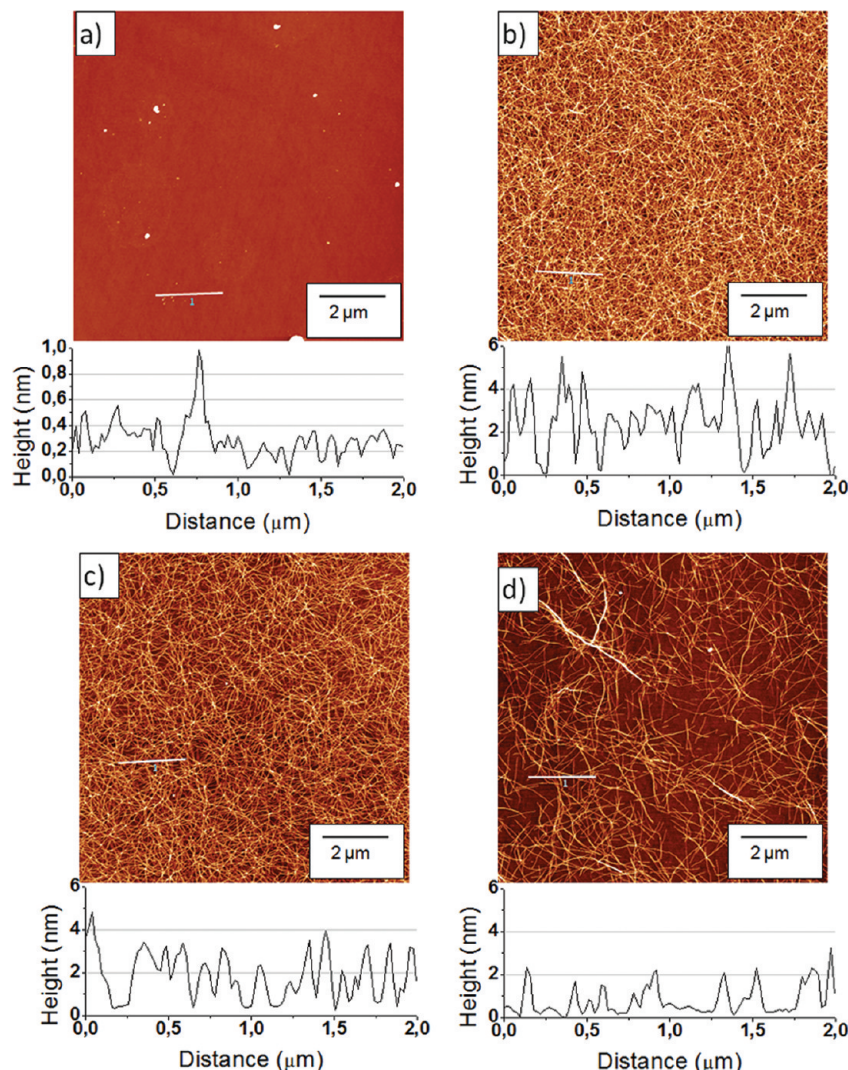


Figure 3. AFM height images and surface profiles of thiol/HAuCl₄ at different thiol to gold precursor ratios. (a) 1 to 1, (b) 3 to 1, (c) 10 to 1, and (d) 20 to 1.

therefore the equilibrium between the two types of interaction is displaced toward the formation of DMF-MPA hydrogen bonds instead of MPA-MPA hydrogen bonds. As a consequence, the particles are surrounded by a DMF shell, preventing the formation of NPCs. Concerning cysteamine, both the amine and the thiol group have a strong affinity to gold. Therefore, the absence of fibers could be due to the adsorption of both the amino groups and the thiol on the gold surface, making the formation of hydrogen bonds impossible.^{40,41} Furthermore, the addition of HAuCl₄ acidifies the solution. As a consequence, the amine group of the cysteamine could be protonated, which would result in an electrostatic repulsion of the particles. To confirm this hypothesis, the pH of the solution was altered by addition of aqueous sodium hydroxide to obtain the noncharged form of the amine. However, since the main solvent is DMF, no exact value of the pH could be obtained. No NPCs were obtained at the higher pH, which could be because the amines preferentially form hydrogen bonds with the DMF. Moreover, the introduction of water in the system could lead to extra hydrogen bonds between the amine and the water molecules, disrupting the formation of the NPCs. In the case of MU, the introduction of a longer carbon chain prevents the formation of fibers. The

longer carbon chain increases the hydrophobicity of the AuNPs and allows crystallization of the ligands surrounding the AuNPs, which results in disordered aggregation of the AuNPs. Concerning BMP, even though the molecule contains a higher number of hydroxyl groups, no NPCs were observed by AFM. In this case, the introduction of branching in the molecule affects the formation of hydrogen bonds. The wedge shaped of the BMP ligand as compared to MEA fills the space at the periphery of the gold cluster more tightly. The higher number of hydroxyl groups per molecule and their closest proximity favors the formation of hydrogen bonds between the ligands of a single particle⁴² and therefore prevents the assembly of nanoparticles.

Investigation of Parameters Affecting the Formation of Fibers. The self-assembly of nanoparticles can be controlled by several types of interaction such as hydrogen bonding, electrostatic interactions, van der Waals interactions, chemical bonding and/or a combination of these forces. These forces are affected by a wide range of parameters such as the surface charge of the particle, the chemical structure of the ligands or the temperature of the system to name a few. In the model described above, the formation of NPCs was attributed to the formation of hydrogen bonds between the hydroxyl groups of

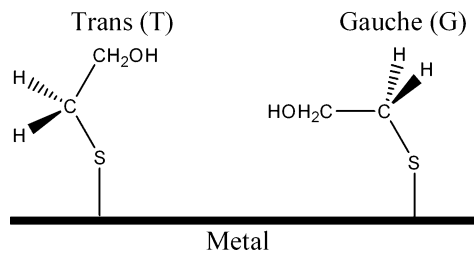
the ligands on the one hand and between the hydroxyl groups of the ligands and the solvent on the other hand. To confirm this model, the effects of molar ratio of thiol to gold precursor, temperature, pH, and solvent on the formation of NPCs have been evaluated.

Effect of Thiol to Gold Precursor Molar Ratio. Molar ratio between thiol and gold precursor was the first parameter investigated. Samples were prepared from an equimolar ratio to up to 50 times excess of thiol. AFM images of thiol/HAuCl₄ solutions spin-coated on silicon substrates are presented in Figure 3. No fibers were observed when an equimolar ratio of thiol to gold precursor was used (Figure 3a), while increasing the amount of thiol up to a 20 times excess resulted in the formation of NPCs (Figure 3). Increasing the amount of thiol even more, up to a 50 times excess, disrupts the formation of NPCs. Interestingly, the thickness of the fibers is independent of the molar ratio between thiol and gold precursor. For instance, fibers of 50–100 nm in thickness are observed for molar ratios of 3:1, 5:1, 10:1, or 20:1 thiol to gold precursor. Raman spectroscopy investigations have shown that the conformation of chemisorbed MEA on gold changes from a gauche conformation to a trans conformation upon addition of thiol, Scheme 2.⁴³ At low concentrations, the density of MEA

available for hydrogen bonding.⁴³ The obtained results suggest that an excess of thiols is crucial to densely cover the gold nanoclusters and therefore to direct their self-assembly into NPCs. However, the introduction of a large excess of thiols disrupts the NPCs formation. The large excess of thiols competes in the formation of hydrogen bonds, hence resulting in the formation of aggregates.³⁶

Effect of Temperature. The effect of temperature on the NPCs stability is an important study related to the hydrogen bond formation between the hybrid building blocks. A closed vial containing NPCs obtained from the self-assembly of MEA stabilized AuNPs in DMF was heated under stirring at either 50 or 100 °C for 1 h. AFM measurements were conducted on samples prepared from the solution directly after heating and after cooling for 24 h. The AFM height images taken from the sample heated at 50 °C are presented in Figure 4. After heating the NPCs at 50 °C for 1 h, the formation of small dots was observed among the particle chains. These dots have the same thickness and height as the NPCs, suggesting that they consist of fragments of NPCs (Figure 4a). After cooling, the dots disappeared and thin (50–100 nm thick) and thick NPCs (up to 200 nm thick) were formed (Figure 4b). On the other hand, AFM measurements performed after heating the solution at 100 °C for 1 h revealed a smooth surface both before and after cooling. No NPCs or dots were observed on the solid substrate at this temperature. These observations suggest that heating the solution at 50 °C brings enough energy to partially break the hydrogen bonds which are holding the hybrid building blocks (nanoparticles) together. After cooling, thicker NPCs are formed due to aggregation between fragments of NPCs via new sets of hydrogen bond. In contrast, heating the solution at 100 °C brings enough energy to completely break the assembly. These results demonstrate that temperature disturbs the formation of NPCs, probably not only by breaking the hydrogen bonds but also by changing the structure of the hybrid building blocks to inhibit the unidirectional morphology. Raman spectroscopy studies have shown that temperature affects the conformation of the adsorbed MEA on a gold surface: higher temperature increases the proportion of gauche MEA. Therefore, the availability of the hydroxyl groups decreases upon heating, which explains the breaking of the

Scheme 2. Representation as the trans and gauche Conformation of MEA, as Described by Kudelski⁴³



molecules adsorbed on the gold surface is low and the molecules can adopt a gauche conformation, lying on the surface. When the concentration of MEA increases, more molecules get adsorbed on the surface and they adapt a linear trans conformation, which makes the hydroxyl groups more

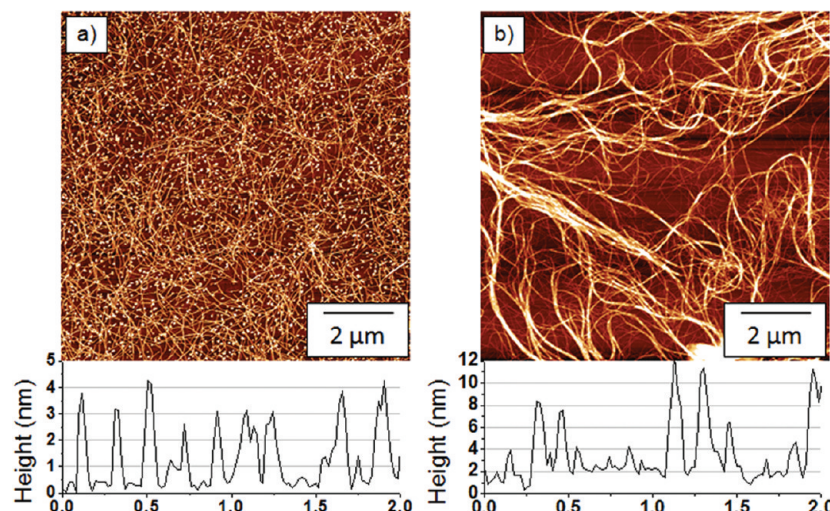


Figure 4. AFM height images and surface profiles of thiol + HAuCl₄ (molar ratio of 5 to 1) after heating for 1 h at 50 °C before (a) and after (b) cooling.

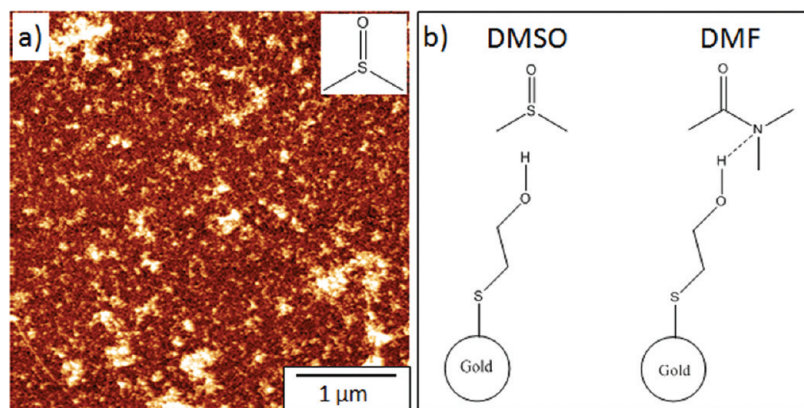


Figure 5. (a) AFM height images of MEA+HAuCl₄ (molar ratio of 5 to 1) in DMSO. (b) Scheme showing the absence of H-bond between the MEA and DMSO and the formation of H-bond between MEA and DMF.

fibers. After cooling, the molecules go back to a trans conformation and some new hydrogen bonds can be formed. Moreover, elevated temperature could promote the oxidative cleavage of the C–S bond, resulting in thiolated nanoparticles.³⁷ To validate this hypothesis, IR spectroscopy was performed on the MEA/HAuCl₄ system before and after heating at 100 °C for 1 h (see the Supporting Information). After heating the solution, the signal at 3648 cm⁻¹ corresponding to the formation of hydrogen bonds disappears, confirming the disruption of the hydrogen bonds. This study further strengthens the presence of hydrogen bonds between the AuNPs and suggests that the NPCs thickness could be tailored by varying the temperature of the NPCs solution (Figure 4b).

Effect of pH. The effect of the acidity of the solution on the stability of the fibers was also evaluated. Even though the pH of a DMF solution cannot be accurately determined with a pH meter, such measures give an indication of the relative acidity of the solution. The thiol and gold precursor solution (molar ratio of 5 to 1) in DMF had a pH of 2.2. The relative acidity of the initial solution is due to the dissociation of the gold precursor into H⁺ and [AuCl₄]⁻. The pH was increased to pH 7, 10, and 14 by addition of an aqueous NaOH solution. AFM measurements were conducted on the different solutions and revealed that NPCs were stable only in acidic pH (pH = 2.2). When decreasing the acidity of the solution, the NPCs were destroyed. Upon addition of aqueous NaOH to the solution, the hydroxyl group of the MEA is partly deprotonated, resulting in a heterogeneous charge distribution. The electrostatic repulsion between the negatively charged particles is causing the disassembly of the NPCs. These results indicate that switching the surface charges of the hybrid nanoparticles via tuning the pH significantly influences the NPCs formation. Interestingly, decreasing the pH of the solution back to its initial value does not permit the reformation of NPCs. One explanation is the introduction of water in the system that can compete in the formation of hydrogen bonds and prevent the alignment of the AuNPs.

Effect of Solvent. The effect of different solvents on the stability of the fibers was also examined. MEA was dissolved in ethanol, water, and DMSO as an alternative to DMF. In water and ethanol, precipitates were formed upon addition of gold precursor, revealing that the particles were not stabilized efficiently by the ligands. In DMSO, the formation of aggregates was observed (Figure 5). A major difference

between DMF and DMSO is the presence of a lone electron pair on the nitrogen atom of the DMF which can participate in hydrogen bonds. Therefore, hydrogen bond formation between the polar solvent and the hybrid building blocks contributes to stabilize and direct the self-assembly of the hybrid building blocks into 1D arrays. The formation of hydrogen bonds between the DMF and the hydroxyl group of the ligand prevent the agglomeration of particles. In the case of DMSO, the hydroxyl groups of the MEA are free to interact with each other and consequently aggregates are formed (Figure 5).

CONCLUSION

A simple and cost-efficient concept to fabricate NPCs based on gold nanoparticles has been presented. The gold particles were prepared *in situ* by reduction of hydrogen tetrachloroaurate as gold precursor in the presence of the commercially available mercaptoethanol. Combining both materials leads to the spontaneous self-assembly of AuNPs into NPCs with well-defined interparticle distance. The formation of hydrogen bonds between the hydroxyl groups of the ligands and between a hydroxyl group of a ligand and the nitrogen atom of the dimethylformamide seem to be key parameters for the direction of the self-assembly into monodimensional arrays. Therefore, the choice of the solvent and the structure of the ligand are of critical importance. To our knowledge, this is a unique single step method reporting the formation of 1D arrays consisting of discrete gold nanoparticles. This approach could be applied to fabricate a wide range of functional hybrid NPCs from different types of metallic, magnetic, and semiconductor nanoparticles leading to a broad spectrum of applications including nanoelectronics, catalysis, nanomedicine, and filtrations.

ASSOCIATED CONTENT

Supporting Information

IR spectra of the MEA/HAuCl₄ solution and AFM images taken for the different ligands and at different pH. This material is available free of charge via the Internet at <http://pubs.acs.org>.

AUTHOR INFORMATION

Corresponding Author

^{*}(M.M.) Telephone: +46 8 790 8768. E-mail: Malkoch@kth.se.
(A.F.) Telephone: +49 2821 806 73 634. E-mail: Amir.Fahmi@hochschule-rhein-waal.de.

Notes

The authors declare no competing financial interest.

ACKNOWLEDGMENTS

The authors are grateful to the Swedish Research Council (VR) for its financial support (Grants 2008-5609, 2006-3617, and 2009-3259) as well as to the UK Engineering and Physical Sciences Research Council (EPSRC) and the Nottingham Innovative Manufacturing Research Centre (NIMRC). The authors also acknowledge the Nanocentre from Nottingham for the HRTEM measurements.

REFERENCES

- (1) Fahmi, A.; Pietsch, T.; Mendoza, C.; Cheval, N. Functional hybrid materials. *Mater. Today* **2009**, *12*, 44–50.
- (2) Grzelczak, M.; Vermant, J.; Furst, E. M.; Liz-Marzan, L. M. Directed Self-Assembly of Nanoparticles. *ACS Nano* **2010**, *4*, 3591–3605.
- (3) Liu, K.; Zhao, N.; Kumacheva, E. Self-assembly of inorganic nanorods. *Chem. Soc. Rev.* **2011**, *40*, 656–671.
- (4) Zhou, S.; Ma, Z.; Baker, G. A.; Rondinone, A. J.; Zhu, Q.; Luo, H.; Wu, Z.; Dai, S. Self-Assembly of Metal Oxide Nanoparticles into Hierarchically Patterned Porous Architectures Using Ionic Liquid/Oil Emulsions. *Langmuir* **2009**, *25*, 7229–7233.
- (5) Anish Kumar, M.; Jung, S.; Ji, T. Protein biosensors based on polymer nanowires, carbon nanotubes and zinc oxide nanorods. *Sensors* **2011**, *11*, 5087–5111.
- (6) Ratto, F.; Matteini, P.; Centi, S.; Rossi, F.; Pini, R. Gold nanorods as new nanochromophores for photothermal therapies. *J. Biophotonics* **2011**, *4*, 64–73.
- (7) Stone, J.; Jackson, S.; Wright, D. Biological applications of gold nanorods. *Wiley Interdiscip. Rev.: Nanomed. Nanobiotechnol.* **2011**, *3*, 100–109.
- (8) Kim, F. S.-J.; Ren, G.-Q.; Jenekhe, S. A. One-Dimensional Nanostructures of π-Conjugated Molecular Systems: Assembly, Properties, and Applications from Photovoltaics, Sensors, and Nanophotonics to Nanoelectronics. *Chem. Mater.* **2011**, *23*, 682–732.
- (9) Kjelstrup-Hansen, J.; Tavares, L.; Hansen, R. M. d. O.; Liu, X.; Bordo, K.; Rubahn, H.-G. Optical properties of microstructured surface-grown and transferred organic nanofibers. *J. Nanophotonics* **2011**, *5*, 051701/1–051701/11.
- (10) Hansen, M. R. d. O.; Madsen, M.; Kjelstrup-Hansen, J.; Rubahn, H.-G. In situ-Directed Growth of Organic Nanofibers and Nanoflakes: Electrical and Morphological Properties. *Nanoscale Res. Lett.* **2010**, *6*, 1–5.
- (11) Hansen, R. M. d. O.; Madsen, M.; Kjelstrup-Hansen, J.; Pedersen, R. H.; Gadegaard, N.; Rubahn, H.-G. Electrical properties of in-situ grown and transferred organic nanofibers. *Proc. SPIE* **2010**, *7764* (Nanoengineering: Fabrication, Properties, Optics, and Devices VII), 77640L/1–77640L/8.
- (12) Haq, S.; Hanke, F.; Dyer, M. S.; Persson, M.; Iavicoli, P.; Amabilino, D. B.; Raval, R. Clean Coupling of Unfunctionalized Porphyrins at Surfaces To Give Highly Oriented Organometallic Oligomers. *J. Am. Chem. Soc.* **2011**, *133*, 12031–12039.
- (13) Yin, Z.; Wang, B.; Chen, G.; Zhan, M. One-dimensional 8-hydroxyquinoline metal complex nanomaterials: synthesis, optoelectronic properties, and applications. *J. Mater. Sci.* **2011**, *46*, 2397–2409.
- (14) Acar, H.; Garifullin, R.; Guler, M. O. Self-assembled template-directed synthesis of one-dimensional silica and titania nanostructures. *Langmuir* **2011**, *27*, 1079–84.
- (15) Greiner, A.; Wendorff, J. H. Electrospinning: a fascinating method for the preparation of ultrathin fibers. *Angew. Chem., Int. Ed.* **2007**, *46*, 5670–5703.
- (16) Huang, Z.-M.; Zhang, Y. Z.; Kotaki, M.; Ramakrishna, S. A review on polymer nanofibers by electrospinning and their applications in nanocomposites. *Compos. Sci. Technol.* **2003**, *63*, 2223–2253.
- (17) DeVries, G. A.; Brunnbauer, M.; Hu, Y.; Jackson, A. M.; Long, B.; Neltner, B. T.; Uzun, O.; Wunsch, B. H.; Stellacci, F. Divalent Metal Nanoparticles. *Science* **2007**, *315*, 358–361.
- (18) Zhang, H.; Fung, K.-H.; Hartmann, J.; Chan, C. T.; Wang, D. Controlled Chainlike Agglomeration of Charged Gold Nanoparticles via a Deliberate Interaction Balance. *J. Phys. Chem. C* **2008**, *112*, 16830–16839.
- (19) Zhang, H.; Wang, D. Controlling the growth of charged-nanoparticle chains through interparticle electrostatic repulsion. *Angew. Chem., Int. Ed.* **2008**, *47*, 3984–3987.
- (20) Pruneau, S.; Olenic, L.; Al-Said, S. A. F.; Borodi, G.; Houlton, A.; Horrocks, B. R. Template and template-free preparation of one-dimensional metallic nanostructures. *J. Mater. Sci.* **2011**, *45*, 3151–3159.
- (21) Lee, J.; Zhou, H.; Lee, J. Small molecule induced self-assembly of Au nanoparticles. *J. Mater. Chem.* **2011**, *21*, 16935–16942.
- (22) Matsukawa, N.; Yamashita, I. Ordered array of gold nanoparticles promoted by functional peptides. *Appl. Phys. Express* **2011**, *4*, 057001/1–057001/3.
- (23) Trabattoni, S.; Moret, M.; Miozzo, L.; Campione, M. Self-assembly of gold nanoparticles on functional organic molecular crystals. *J. Colloid Interface Sci.* **2011**, *360*, 422–429.
- (24) Beverina, L. Towards the Controlled Self-Assembly of Gold Nanoparticles. *ChemPhysChem* **2010**, *11*, 2075–2077.
- (25) Qiao, Y.; Chen, H.; Lin, Y.; Huang, J. Controllable Synthesis of Water-Soluble Gold Nanoparticles and Their Applications in Electrocatalysis and Surface-Enhanced Raman Scattering. *Langmuir* **2011**, *27*, 11090–11097.
- (26) Dubavik, A.; Lesnyak, V.; Gaponik, N.; Eychmuller, A. One-Phase Synthesis of Gold Nanoparticles with Varied Solubility. *Langmuir* **2011**, *27*, 10224–10227.
- (27) Lau, C. Y.; Duan, H.; Wang, F.; He, C. B.; Low, H. Y.; Yang, J. K. W. Enhanced Ordering in Gold Nanoparticles Self-Assembly through Excess Free Ligands. *Langmuir* **2011**, *27*, 3355–3360.
- (28) Daniel, M.-C.; Astruc, D. Gold Nanoparticles: Assembly, Supramolecular Chemistry, Quantum-Size-Related Properties, and Applications toward Biology, Catalysis, and Nanotechnology. *Chem. Rev.* **2004**, *104*, 293–346.
- (29) Feng, L.; Gao, G.; Huang, P.; Wang, K.; Wang, X.; Luo, T.; Zhang, C. Optical properties and catalytic activity of bimetallic gold-silver nanoparticles. *Nano Biomed. Eng.* **2010**, *2*, 258–267.
- (30) Vidotti, M.; Carvalhal, R. F.; Mendes, R. K.; Ferreira, D. C. M.; Kubota, L. T. Biosensors based on gold nanostructures. *J. Braz. Chem. Soc.* **2011**, *22*, 3–20.
- (31) Pissuwan, D.; Niidome, T.; Cortie, M. B. The forthcoming applications of gold nanoparticles in drug and gene delivery systems. *J. Controlled Release* **2011**, *149*, 65–71.
- (32) Uehara, N. Polymer-functionalized gold nanoparticles as versatile sensing materials. *Anal. Sci.* **2010**, *26*, 1219–1228.
- (33) Turkevich, J.; Stevenson, P. C.; Hillier, J. The nucleation and growth processes in the synthesis of colloidal gold. *Discuss. Faraday Soc.* **1951**, *55*–75.
- (34) Brust, M.; Walker, M.; Bethell, D.; Schiffrin, D. J.; Whyman, R. Synthesis of thiol-derivatised gold nanoparticles in a two-phase Liquid-Liquid system. *J. Chem. Soc., Chem. Commun.* **1994**, *7*, 801–802.
- (35) Chen, S.; Murray, R. W. Arenethiolate Monolayer-Protected Gold Clusters. *Langmuir* **1998**, *15*, 682–689.
- (36) Lin, S.; Li, M.; Dujardin, E.; Girard, C.; Mann, S. One-dimensional plasmon coupling by facile self-assembly of gold nanoparticles into branched chain networks. *Adv. Mater. (Weinheim, Ger.)* **2005**, *17*, 2553–2559.
- (37) Li, M.; Johnson, S.; Guo, H.; Dujardin, E.; Mann, S. A Generalized Mechanism for Ligand-Induced Dipolar Assembly of Plasmonic Gold Nanoparticle Chain Networks. *Adv. Funct. Mater.* **2011**, *21*, 851–859.
- (38) Kanno, H.; Honshoh, M.; Yoshimura, Y. Free hydrogen bonds in alcohol solutions with inert solvents. *J. Solution Chem.* **2000**, *29*, 1007–1016.
- (39) Nandy, S. K.; Mukherjee, D. K.; Roy, S. B.; Kastha, G. S. Vibrational spectra and rotational isomerism in 2-mercaptoethanol. *Can. J. Chem.* **1973**, *51*, 1139–41.

- (40) Kudelski, A.; Hill, W. Raman Study on the Structure of Cysteamine Monolayers on Silver. *Langmuir* **1999**, *15*, 3162–3168.
- (41) Lee, H.; Kim, M. S.; Suh, S. W. Raman spectroscopy of sulfur-containing amino acids and their derivatives adsorbed on silver. *J. Raman Spectrosc.* **1991**, *22*, 91–6.
- (42) Paulini, R.; Frankamp, B. L.; Rotello, V. M. Effects of Branched Ligands on the Structure and Stability of Monolayers on Gold Nanoparticles. *Langmuir* **2002**, *18*, 2368–2373.
- (43) Kudelski, A. Chemisorption of 2-Mercaptoethanol on Silver, Copper, and Gold: Direct Raman Evidence of Acid-Induced Changes in Adsorption/Desorption Equilibria. *Langmuir* **2003**, *19*, 3805–3813.